Supporting Information

Advanced Operation of Heated Fluidic Resonators via Mechanical and Thermal Loss Reduction in Vacuo

Juhee Ko, Bong Jae Lee & Jungchul Lee¶

Center for Extreme Thermal Physics and Manufacturing, Department of Mechanical Engineering, Korea Advanced Institute of Science and Technology (KAIST), 34141, Daejeon-si, Korea

¶*Corresponding Author*

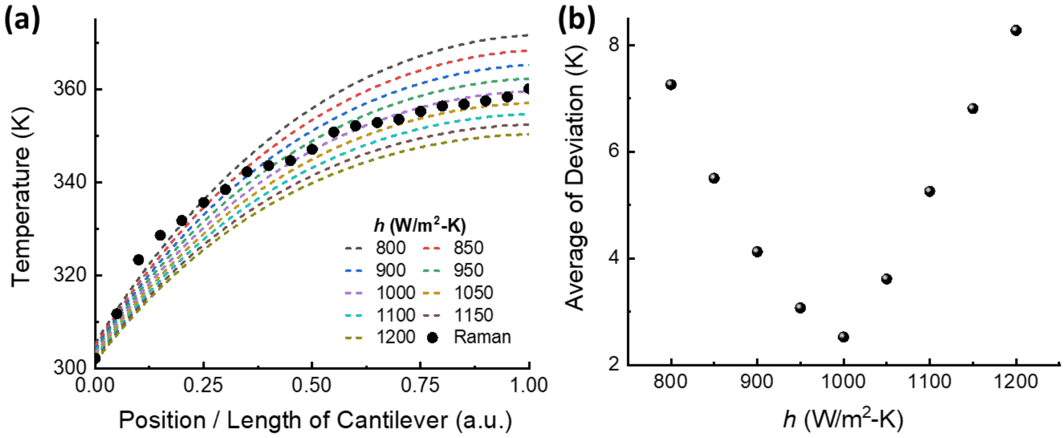

Figure S1. (a) Comparison of the temperature of HFR along channel length (normalized position from the suspended to the free end) from FEM analysis at different convective heat transfer coefficients and Raman thermometry[S1–S3]. Larger deviation in clamped base is due to undercut of silicon nitride insulation layer. (b) Average of the temperature difference between FEM analysis and Raman thermometry as a function of convective heat transfer coefficients.

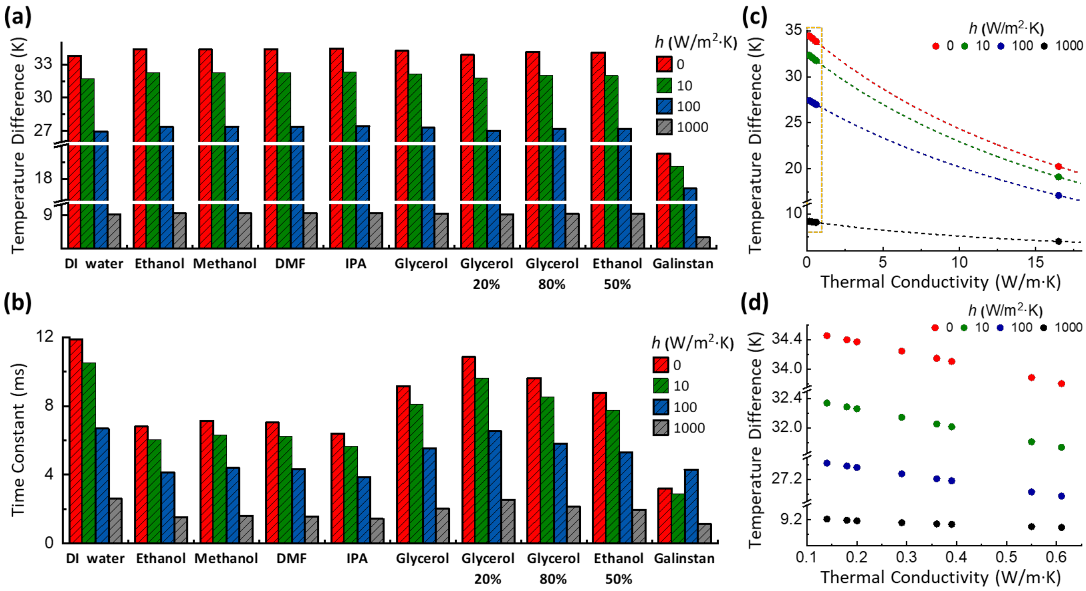

Figure S2. (a) Temperature differences and (b) time constants of the HFR filled with various liquid samples under a 10-mW heating pulse with different convective heat transfer coefficients of 0, 25, and 1000 $W/m^2 \cdot K$. (c) Temperature differences of the HFR filled with various samples as a function of thermal conductivity and (d) its zoomed-in. All data are obtained from transient FEM heat transfer simulation.

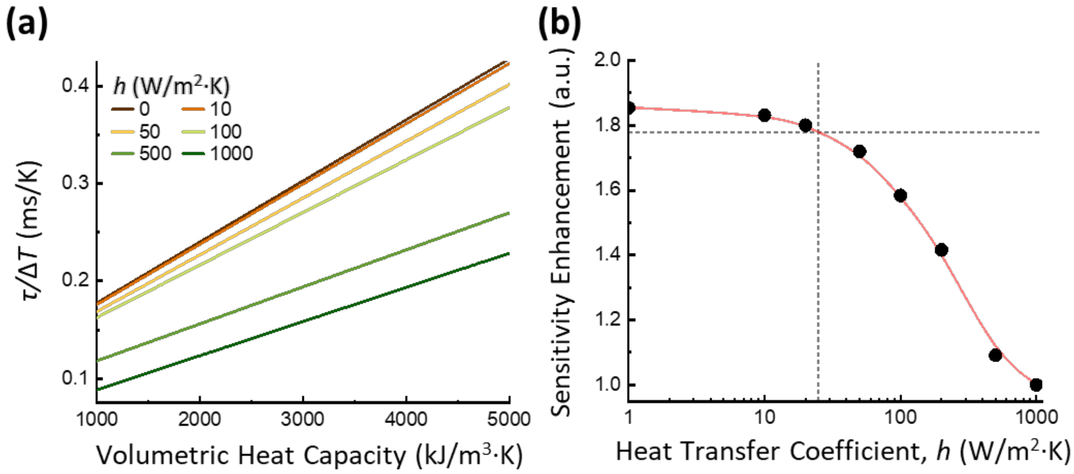

Figure S3. (a) Transient heat transfer FEM simulation showing time constant divided by temperature difference as a function of volumetric heat capacity for different convective heat transfer coefficients. (b) Sensitivity enhancements for volumetric heat capacity measurement calculated as a ratio of sensitivity, slope in (a), at a specific heat transfer coefficient to that at 1000 $W/m^2{\cdot}K$ as a function of convective heat transfer coefficient.

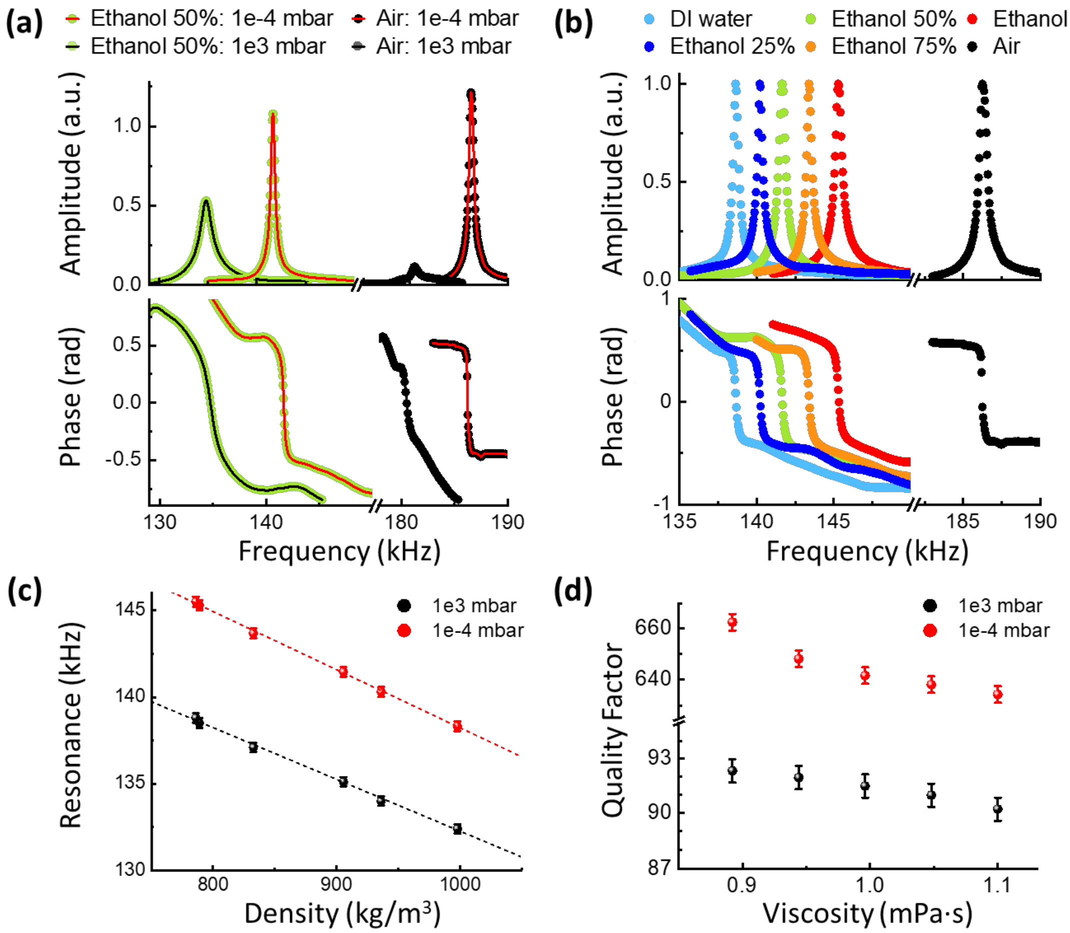

Figure S4. (a) Amplitude spectra of the HFR filled with an ethanol-water binary mixture (50:50 in volume) and air in atmospheric and vacuum pressures (1e3 and 1e-4 mbar, respectively). (b) Amplitude and phase spectra of the HFR filled with various ethanol-water binary mixtures in vacuum pressure (1e-4 mbar). (c) Resonance frequency of the HFR as a function of liquid mass density and (d) quality factor of the HFR as a function of liquid viscosity in atmospheric and vacuum pressures (1e3 and 1e-4 mbar, respectively).

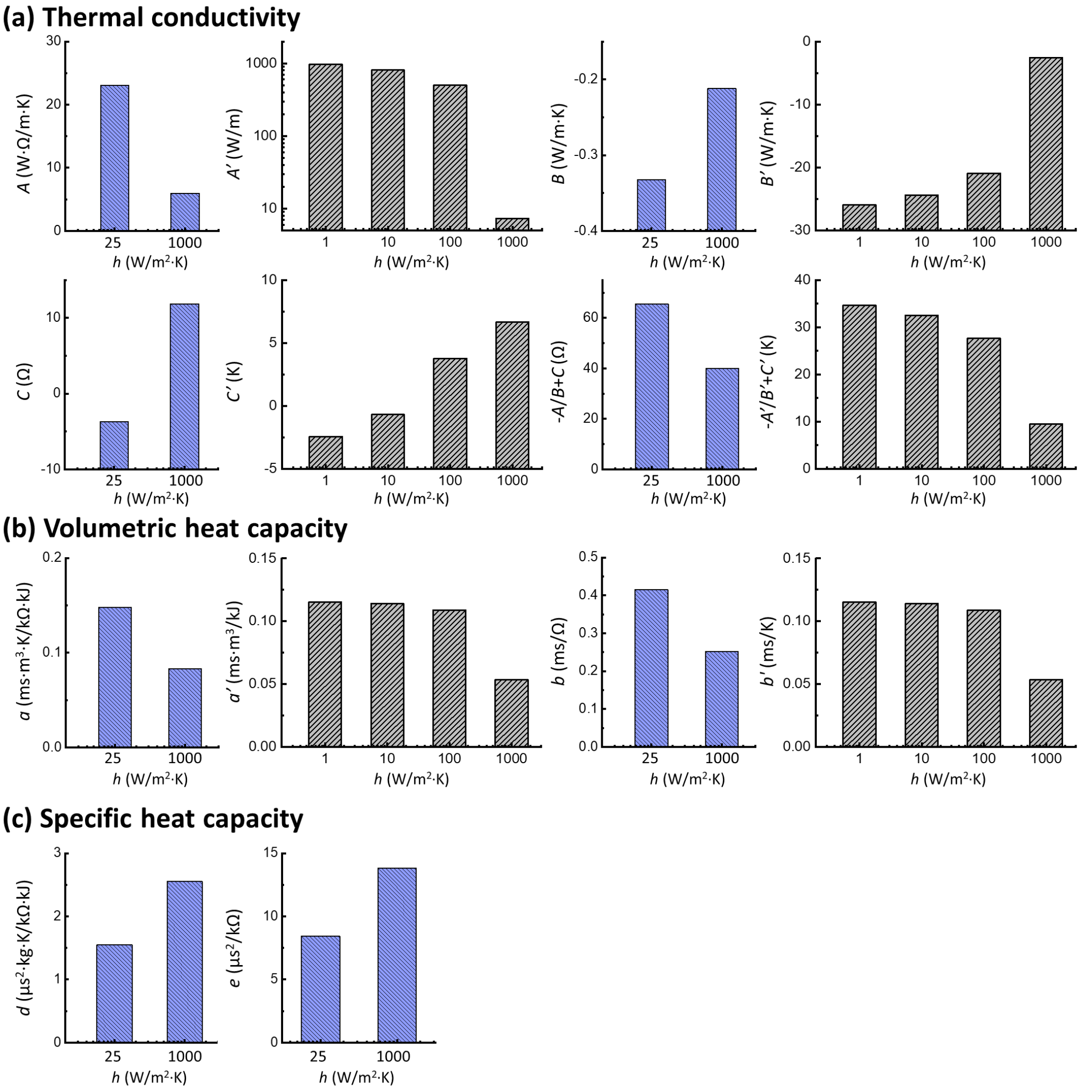

Figure S5. (a) Curve fitting coefficients for thermal conductivity measurement from (experiments) $\Delta T = A/(k\text{-}B)+C$ and (FEA) $\Delta R = A'/(k\text{-}B')+C'$ where T is temperature, R is resistance, and k is thermal conductivity. Trends of horizontal asymptote, C (when $k\rightarrow\infty$), in calibration curves for thermal conductivity show a counter-intuitive decrease with an increasing vacuum (decreasing heat transfer coefficient). Trends of y-intercept, $-A/B+C$ (when $k = 0$), show an increase with vacuum, owing to decreasing thermal loss through ambience during the specific power modulation. (b) Curve fitting coefficients for volumetric heat capacity measurement from (experiments) $\tau/\Delta T=a\cdot\rho c_p+b$ and (FEA) $\tau/\Delta R=a'\cdot\rho c_p+b'$ where τ is time constant and ρc_p is volumetric heat capacity. (c) Curve fitting coefficients for specific heat capacity measurement from $\tau/\Delta R/|\Delta f| =d\cdot\rho c_p+e$.

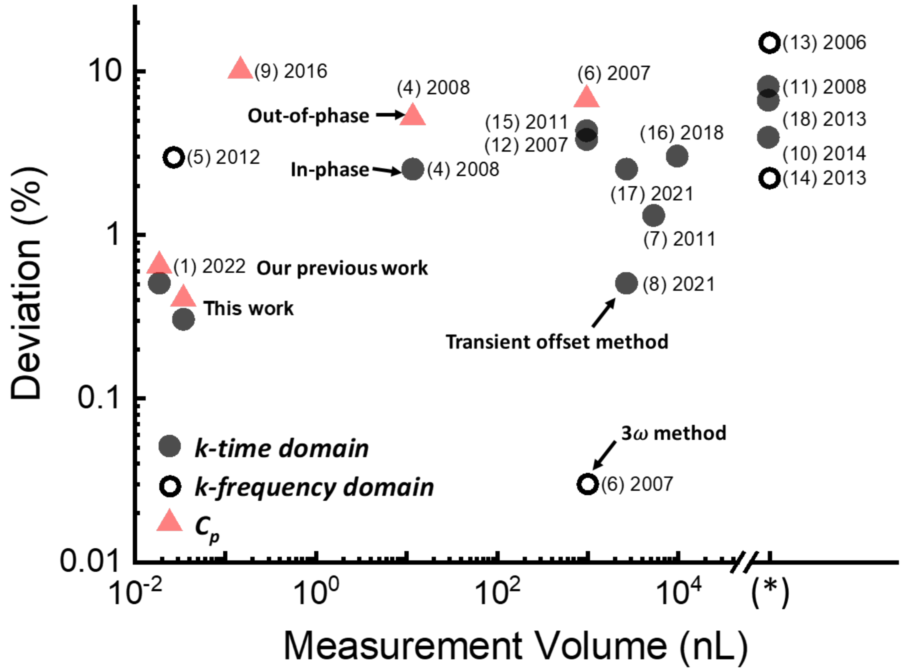

Figure S6. The average deviation of thermal conductivity and heat capacity by using HFR in vacuum environment, compared to the state-of-the-art of thermophysical properties measurements with micro thermal sensors from our previous result[S1] and the other references[S4–S18]. References in (*) use the methods which are hard to define the measurement volume. The HFR with a different length from the previous work is used in this work. Studies so far have been developed by random introduction of new metrologies rather than improving performance.

References for Supporting Information

(1) Ko, J.; Khan, F.; Nam, Y.; Lee, B. J.; Lee, J. Nanomechanical Sensing Using Heater-Integrated Fluidic Resonators. *Nano Lett.* **2022**, *22* (19), 7768–7775. https://doi.org/10.1021/acs.nanolett.2c01572.

(2) Beechem, T.; Graham, S.; Kearney, S. P.; Phinney, L. M.; Serrano, J. R. Invited Article: Simultaneous Mapping of Temperature and Stress in Microdevices Using Micro-Raman Spectroscopy. *Rev. Sci. Instrum.* **2007**, *78* (6), 061301. https://doi.org/10.1063/1.2738946.

(3) Lee, J.; Beechem, T.; Wright, T. L.; Nelson, B. A.; Graham, S.; King, W. P. Electrical, Thermal, and Mechanical Characterization of Silicon Microcantilever Heaters. *J. Microelectromech. Syst.* **2006**, *15* (6), 1644–1655. https://doi.org/10.1109/JMEMS.2006.886020.

(4) Choi, S. R.; Kim, D. Real-Time Thermal Characterization of 12 nl Fluid Samples in a Microchannel. *Rev. Sci. Instrum.* **2008**, *79* (6), 064901. https://doi.org/10.1063/1.2937180.

(5) Park, B. K.; Yi, N.; Park, J.; Kim, D. Note: Development of a Microfabricated Sensor to Measure Thermal Conductivity of Picoliter Scale Liquid Samples. *Rev. Sci. Instrum.* **2012**, *83* (10), 106102. https://doi.org/10.1063/1.4757400.

(6) Choi, S. R.; Kim, J.; Kim, D. 3ω Method to Measure Thermal Properties of Electrically Conducting Small-Volume Liquid. *Rev. Sci. Instrum.* **2007**, *78* (8), 084902. https://doi.org/10.1063/1.2777162.

(7) Kuvshinov, D.; Bown, M. R.; MacInnes, J. M.; Allen, R. W. K.; Ge, R.; Aldous, L.; Hardacre, C.; Doy, N.; Newton, M. I.; McHale, G. Thermal Conductivity Measurement of Liquids in a Microfluidic Device. *Microfluid. Nanofluidics* **2011**, *10* (1), 123–132. https://doi.org/10.1007/s10404-010-0652-x.

(8) Oudebrouckx, G.; Vandenryt, T.; Bormans, S.; Wagner, P. H.; Thoelen, R. Measuring Thermal Conductivity in a Microfluidic Device with the Transient Thermal Offset (TTO) Method. *IEEE Sens. J.* **2021**, *21* (6), 7298–7307. https://doi.org/10.1109/JSEN.2020.3047475.

(9) Khan, M. F.; Miriyala, N.; Lee, J.; Hassanpourfard, M.; Kumar, A.; Thundat, T. Heat Capacity Measurements of Sub-Nanoliter Volumes of Liquids Using Bimaterial Microchannel Cantilevers. *Appl. Phys. Lett.* **2016**, *108* (21), 211906. https://doi.org/10.1063/1.4952614.

(10) Kujawska, T.; Secomski, W.; Kruglenko, E.; Krawczyk, K.; Nowicki, A. Determination of Tissue Thermal Conductivity by Measuring and Modeling Temperature Rise Induced in Tissue by Pulsed Focused Ultrasound. *PLoS One* **2014**, *9* (4), e94929. https://doi.org/10.1371/journal.pone.0094929.

(11) Zhu, S.; Marcotte, M.; Ramaswamy, H.; Shao, Y.; Le-Bail, A. Evaluation and Comparison of Thermal Conductivity of Food Materials at High Pressure. *Food Bioprod. Process* **2008**, *86* (3), 147–153. https://doi.org/10.1016/j.fbp.2006.08.001.

(12) Choi, S. R.; Kim, D. Measurement of Thermal Properties of Microfluidic Samples Using Laser Point Heating Thermometry. *Thermochim. Acta* **2007**, *455*, 11–15. https://doi.org/10.1016/j.tca.2006.11.035.

(13) Kuntner, J.; Kohl, F.; Jakoby, B. Simultaneous Thermal Conductivity and Diffusivity Sensing in Liquids Using a Micromachined Device. *Sens. Actuators A, Phys.* **2006**, *130–131*, 62–67. https://doi.org/10.1016/j.sna.2005.11.021.

(14) Gauthier, S.; Giani, A.; Combette, P. Gas Thermal Conductivity Measurement Using the Three-Omega Method. *Sens. Actuators A, Phys.* **2013**, *195*, 50–55. https://doi.org/10.1016/j.sna.2012.12.032.
(15) Yi, N.; Park, B. K.; Kim, D.; Park, J. Micro-Droplet Detection and Characterization Using Thermal Responses. *Lab. Chip* **2011**, *11* (14), 2378–2384. https://doi.org/10.1039/c0lc00728e.
(16) Shrestha, R.; Atluri, R.; Simmons, D. P.; Kim, D. S.; Choi, T. Y. A Micro-Pipette Thermal Sensing Technique for Measuring the Thermal Conductivity of Non-Volatile Fluids. *Rev. Sci. Instrum.* **2018**, *89* (11), 114902. https://doi.org/10.1063/1.5044214.
(17) Oudebrouckx, G.; Nieder, D.; Vandenryt, T.; Bormans, S.; Möbius, H.; Thoelen, R. Single Element Thermal Sensor for Measuring Thermal Conductivity and Flow Rate inside a Microchannel. *Sens. Actuators A, Phys.* **2021**, *331*, 112906. https://doi.org/10.1016/j.sna.2021.112906.
(18) Shrestha, R.; Lee, K. M.; Chang, W. S.; Kim, D. S.; Rhee, G. H.; Choi, T. Y. Steady Heat Conduction-Based Thermal Conductivity Measurement of Single Walled Carbon Nanotubes Thin Film Using a Micropipette Thermal Sensor. *Rev. Sci. Instrum.* **2013**, *84* (3), 034901. https://doi.org/10.1063/1.4792841.